Title

Functional Effects of Cuprizone-Induced Demyelination in the Presence of the mTOR-Inhibitor Rapamycin

Authors

Yamate-Morgan, Hana
Lauderdale, Kelli
Horeczko, Joshua
et al.

Publication Date

2019-05-01

DOI

10.1016/j.neuroscience.2019.01.038

Peer reviewed

HHS Public Access

Author manuscript

Neuroscience. Author manuscript; available in PMC 2019 August 06.

Published in final edited form as:

Neuroscience. 2019 May 15; 406: 667–683. doi:10.1016/j.neuroscience.2019.01.038.

Functional Effects of Cuprizone-Induced Demyelination in the Presence of the mTOR-Inhibitor Rapamycin ⋆,„⋆⋆

Hana Yamate-Morgan[a,b,†], **Kelli Lauderdale**[b,†], **Joshua Horeczko**[b], **Urja Merchant**[b], **Seema K. Tiwari-Woodruff**[a,b,c,*]

[a]Department of Neuroscience, University of California, Riverside (UCR), Riverside, CA 92521, USA

[b]Division of Biomedical Sciences, UCR School of Medicine, Riverside, CA 92521, USA

[c]Center for Glial-Neuronal Interactions, UCR School of Medicine, CA 92521

Abstract

Persistent demyelination has been implicated in axon damage and functional deficits underlying neurodegenerative diseases such as multiple sclerosis. The cuprizone diet model of demyelination allows for the investigation of mechanisms underlying timed and reproducible demyelination and remyelination. However, spontaneous oligodendrocyte (OL) progenitor (OPC) proliferation, OPC differentiation, and axon remyelination during cuprizone diet may convolute the understanding of remyelinating events. The Akt (a serine/threonine kinase)/mTOR (the mammalian target of rapamycin) signaling pathway in OLs regulates intermediate steps during myelination. Thus, in an effort to inhibit spontaneous remyelination, the mTOR inhibitor rapamycin has been administered during cuprizone diet. Intrigued by the potential for rapamycin to optimize the cuprizone model by producing more complete demyelination, we sought to characterize the effects of rapamycin on axonal function and myelination. Functional remyelination was assessed by callosal compound action potential (CAP) recordings along with immunohistochemistry in mice treated with rapamycin during cuprizone diet. Rapamycin groups exhibited similar myelination, but significantly increased axonal damage and inflammation compared to non-rapamycin groups. There was minimal change in CAP amplitude between groups, however, a significant decrease in conduction velocity of the slower, non-myelinated CAP component was observed in the rapamycin group relative to the non-rapamycin group. During remyelination, rapamycin groups showed a significant decrease in OPC proliferation and mature OLs, suggesting a delay in OPC differentiation kinetics. In conclusion, we question the use of rapamycin to produce consistent demyelination as rapamycin increased inflammation and axonal damage, without affecting myelination.

⋆⋆Competing Financial Interests: The authors declare that they have no competing financial interests.

*Corresponding author at: Division of Biomedical Sciences, School of Medicine, University of California Riverside, Room 205, 311 School of Medicine Research Building, 900 University Ave, Riverside, CA 92521, USA. Tel.: +1 951 827 7819. seema.tiwari-woodruff@medsch.ucr.edu (Seema K. Tiwari-Woodruff).

⋆Author Contributions: SKTW conceived of and supervised the study. HYM, JH, and KL performed experiments. SKTW, HYM, KL, JM, and UM analyzed the data; HYM, KL, and SKTW wrote the manuscript.

†HYM and KL contributed equally and should be considered first co-authors.

Keywords

oligodendrocyte; demyelination; cuprizone diet; axon damage; compound action potential; remyelination

INTRODUCTION

Demyelination can be achieved using many well-established mouse models of multiple sclerosis (MS), including experimental autoimmune encephalomyelitis (EAE), cuprizone diet (CPZ), lysolecithin and ethidium bromide focal injections (Denic et al., 2011; McCarthy et al., 2012; Ransohoff, 2012). The most common model of MS is EAE as it recapitulates the inflammatory, demyelinating, and neurodegenerative aspects of MS pathology (Sternberger et al., 1984; Wekerle et al., 1994; Baxter, 2007; Mangiardi et al., 2011; Hasselmann et al., 2017). Cuprizone is toxic to mature oligodendrocytes (OLs) without causing direct neuronal damage and produces consistent demyelination in both white and gray matter within the central nervous system (CNS) (Matsushima and Morell, 2001; Blakemore and Franklin, 2008). Thus, the CPZ model is routinely used to understand molecular mechanism of de- and remyelination and screen remyelinating therapeutic agents.

While the mechanisms of cuprizone-induced demyelination are not well understood, it has been hypothesized that it disrupts energy metabolism in mature OLs leading to apoptosis (Matsushima and Morell, 2001; Bénardais et al., 2013). However, even in the continued presence of cuprizone, remaining OLs, as well as proliferation and differentiation of OL progenitor cells (OPCs) into myelinating OLs, drives spontaneous remyelination. This spontaneous remyelination is incomplete and this phenomenon has the potential to confound studies assessing the efficiency of remyelinating compounds.

To address this, several eminent research groups have introduced the use of rapamycin along with cuprizone diet (Narayanan et al., 2009; Bai et al., 2016). Rapamycin inhibits the serine/threonine protein kinase mammalian target of rapamycin (mTOR). mTOR is part of the phosphatidyl inositol 3 kinase/protein kinase B (PI3K/Akt) signaling pathway and is critical for OPC/OL survival, proliferation, and differentiation (Tyler et al., 2009; Guardiola-Diaz et al., 2012; Dai et al., 2014; Wahl et al., 2014). mTOR forms the subunit of two heteromeric and functionally distinct complexes, known as mTOR Complex 1 (mTORC1) and 2 (mTORC2) and is part of a complex second messenger signaling that regulates cell proliferation and differentiation (Wood et al., 2013; Dai et al., 2014; Lipton and Sahin, 2014). The primary role of rapamycin in processes specific to OLs depends on a careful balance of activation and action ofmTORC1 (Lebrun-Julien et al., 2014), shown to be a positive regulator of late-stage OPC differentiation, active myelination, and potentially also the local translation of myelin mRNAs, such as myelin basic protein (MBP) (Bercury et al., 2014).

Our group has been investigating novel remyelinating therapeutics using both EAE and cuprizone models. We address remyelination events using behavior, immunohistochemistry (IHC), electron microscopy and electrophysiology to further understand axon pathology and functional remyelination. Recognizing the potential for rapamycin to optimize the cuprizone

model by producing more complete demyelination, we sought to characterize the effects of rapamycin treatment during cuprizone diet on axonal conduction and myelination in the largest white matter tract in the brain, the corpus callosum (CC), that is coherently affected by CPZ diet (Patel et al., 2013; Moore et al., 2014; Hasselmann et al., 2017; Lapato et al., 2017; Karim et al., 2018). In this study, mice were divided between three groups: normal diet (ND), demyelination (CPZ), and remyelination (CPZ + ND). Within the demyelination group, mice were fed 0.2% cuprizone, with or without 10 mg/kg intraperitoneal injections of rapamycin (CPZ + Rapa), for 4.5 weeks and 1.5 weeks. The remyelination group initially followed the same paradigm as the demyelination group (CPZ versus CPZ + Rapa), but was then switched to normal diet for 3 weeks of remyelination ([CPZ] + 3ND versus [CPZ + Rapa] + 3ND). To assess pathological changes in myelination, inflammation, and axon damage during cuprizone diet with rapamycin administration, IHC was performed with the antibodies provided in Table 1. To determine the functional consequences of including rapamycin during cuprizone diet, compound action potentials (CAPs) were recorded across the CC from acute coronal slices. Our examination of the effects of rapamycin treatment during cuprizone administration revealed increased inflammation and callosal axon damage without altering myelin levels during demyelination and remyelination. However, the presence of rapamycin worsened functional and histopathological indicators of axonal pathology. Given these findings, caution should be used when determining whether or not to include rapamycin for functional studies of myelination and interpreting therapeutic effects.

EXPERIMENTAL PROCEDURES

Animals

All procedures and experiments were conducted according to the guidelines established by the American Veterinary Medical Association and the National Institutes of Health and were approved by the Institutional Animal Care and Use Committee (IACUC) of the University of California, Riverside (UCR). Seven-week-old male C57BL/6 mice were obtained from Harlan Laboratories and maintained in-house at the UCR animal facility. Animals were allowed to acclimate for one full week at five animals per cage with standard light/dark cycles.

Cuprizone and Rapamycin Administration

Mice were fed 0.2% cuprizone [oxalic bis(cyclohexylidenehydrazide)] (*Envigo*, Madison, WI) pellets for 4.5 weeks, as previously described (Crawford et al., 2009a,b). Rapamycin (99 + %, *Thermo Fisher Scientific* Waltham, MA cat# J62473) administration was modified from an existing protocol, including its dissolution into 100% methanol, according to its specified solubility at a high concentration (25 mg/mL) in methanol, as compared to less than 2 mg/mL in ethanol. This rapamycin stock was then stored at −20 °C until its dilution in 5% PEG-400, 5% Tween 80, and 4% ethanol just prior to injection. Rapamycin was administered by 0.1 mL intraperitoneal injection at 10 mg/kg body weight per day, five days per week for the duration of the 4.5-week demyelination period, with weights recorded weekly.

Tissue Fixation and Processing

At designated time points and the conclusion of the experiment, mice were deeply anesthetized by inhalation of isoflurane (*Henry Schein* 66,794–017-25 Melville, NY) and transcardially perfused first with phosphate buffered saline (PBS) and then with 10% formalin (*Thermo Fisher Scientific* SF100–20 Waltham, MA). Brains were extracted and post-fixed in 10% formalin for 2 h. Brains were cryoprotected in PBS with 30% sucrose for 48 h and embedded in gelatin for sectioning. Coronal sections (40 μm) were prepared using a HM525 NX cryostat (*Thermo Fisher Scientific* Waltham, MA).

Immunohistochemistry

Coronal brain sections (bregma +0.85 to +0.95 mm, plates 23–24) with CC but no hippocampus (rostral slices) or sections (bregma −1.90 to −2.0 mm, plates 47–48) containing medial hippocampus (caudal slices) were used (Paxinos and Franklin, 2012; Karim et al., 2018). The brain slices were permeabilized, blocked in normal goat serum, and immunolabeled with primary antibodies shown in Table 1. Fluorophore-conjugated (Goat anti-Rabbit Alexa Fluor 555 or 647, *Thermo Fisher Scientific* Waltham, MA) secondary antibodies were used to detect immunolabeled cells. Following detection, cell nuclei were counterstained with 4′,6-diamidino-2-phenylindole (DAPI; 2 ng/mL; *Molecular Probes* D1306 Eugene, OR) and sections were mounted onto glass slides and cover-slipped with Fluoromount G mounting medium (*Thermo Fisher Scientific* 00–4958-02 Waltham, MA) for analysis.

Microscopy and Quantification

Images were acquired using an Olympus BX61 confocal microscope (*Olympus America Inc.*, Center Valley, PA). A single 10× or 20× image, or two 40× images, were taken from the CC per brain section, with two sections analyzed per mouse. Z-stack projections (~20 μm thick) were exported and quantified using ImageJ version 2.2.0-rc-46/1.50 g (NIH) to adjust brightness, contrast and threshold, followed by density analysis (% area) and the use of the multi-point tool to reflect positive immunoreactivity in the CC. IHC analysis generated values of (i) intensity or (ii) density of labeled cells per square millimeter in ImageJ. Intensity was measured in images taken at 20×, centered on the CC of one rostral and one caudal section per mouse after outlining the CC using the polygon tool. Cells were counted in two 40× images of the CC, one rostral and one caudal section per mouse. In each image, cells were counted by splitting channels, applying a threshold color for each channel of interest, and then merging channels to assess overlap between markers of interest (namely, Olig2 and Ki67). The DAPI channel was used to distinguish background staining from labeled cells. For counting cells, the Grid tool (200,000 pixels^2) was applied, and 10 boxes falling within the area of the CC were marked using the multipoint tool. Then, the number of points were then divided by the area (mm^2, converted from pixels^2) within the boxes counted.

Electrophysiology

CAPs were recorded across the CC as previously described (Crawford et al., 2009a,b). Coronal brain slices corresponding approximately to plates 29–48 in the atlas of Paxinos and

Franklin (2012) were prepared from adult (3–4 months) old C57BL/6. Briefly, mice were deeply anesthetized by isoflurane inhalation, decapitated, and the isolated brain was submerged in slicing buffer containing (in mM): 87 NaCl, 75 sucrose 2.5 KCl, 0.5 $CaCl_2$, 7 $MgCl_2$, 1.25 NaH_2-PO_4, 25 $NaHCO_3$, 10 glucose, 1.3 ascorbic acid, 0.1 kynurenic acid, 2.0 pyruvate, and 3.5 MOPS, bubbled with 5% CO_2 + 95% O_2 (Lauderdale et al., 2015). Coronal slices (350 μm) were prepared using a Leica VT 1000S Vibratome (Bannockburn, IL), specified for IHC, and subsequently incubated for 45 min at 35 °C then 15 min at room temperature (24–26 °C). Slices were then transferred to artificial cerebrospinal fluid (ACSF) oxygenated with 5% CO_2 + 95% O_2 containing (in mM): 125 NaCl, 2.5 KCl, 2.5 $CaCl_2$, 1.3 $MgCl_2$, 1.25 NaH_2PO_4, 26.0 $NaHCO_3$, and 15 glucose. Slices were equilibrated in ACSF for a minimum of 15–20 min prior to recording CAPs.

During recording, slices were continuously perfused at room temperature with oxygenated ACSF maintained at a flow rate of 1 mL/min. Recordings were obtained using a Multiclamp 700B Amplifier connected to an Axon Digidata 1550 controlled by PClamp 10.4 Software (*Molecular Devices*, Sunnyvale, CA). Recordings were low-pass filtered at 10 kHz and digitized at 200 kHz. To stimulate CC fibers, a concentric bipolar stimulating electrode (*FHC Neural microTargeting Worldwide*, Bowdoin, ME, USA) was placed approximately 1 mm across from the recording electrode, a glass micropipette with a resistance of 1–3 MΩ (Figs. 9Ai, 10Ai). CAPs were elicited using an episodic stimulation protocol consisting of eight consecutive sweeps, 12 ms in duration, with a 5 s delay between sweeps and an immediate stimulus (0.01 ms duration) after the start of each sweep (Crawford et al., 2009a). Stimulus intensity was adjusted manually using a ISO-Flex stimulator (*A.M.P.I*). Standardized input–output plots were generated in current clamp mode for each slice by averaging at least 4 consecutive sweeps together to reduce the signal-to-noise ratio. CAPs were analyzed using Clampfit 10.4 software (*Molecular Devices*, Sunnyvale, CA), OriginPro 2016 64Bit (OriginLab Corporation) and GraphPad Prism 6 (GraphPad Software) for averaged stimulus responses and latency as previously described (Crawford et al., 2009a).

Statistics

IHC—Brain tissue was collected from n = 5–8 mice per group, from a combination of two separate experiments. Statistics were performed using GraphPad Prism 6 software. Five comparisons were made, as shown between the following groups: (i) ND & CPZ, (ii) CPZ & CPZ + Rapa, (iii) CPZ & [CPZ] + 3 ND, (iv) CPZ + Rapa & [CPZ + Rapa] + 3ND & (v) [CPZ] + 3ND & [CPZ + Rapa] + 3ND. One-way ANOVAs with Tukey's post hoc test for multiple comparisons were used to generate p-values. Data are presented as mean ± SEM, with $p \leq 0.05$ considered statistically significant. In the case that data violated the one-way ANOVA assumption for an approximately Gaussian distribution, the Kruskal-Wallis non-parametric test was used as an alternative to reduce the like-lihood of committing a Type I error.

CAPs—CC CAPs were quantified from at least seven rostral and eight caudal sections (1–2 slices from n = 4–6 mice per group). The peak amplitude of the N1 and N2 components of the CAPs were analyzed for statistical significance using ANOVAs along with Holm-Sidak post hoc tests for multiple comparisons. Statistical analysis of the N2 peak latency was

analyzed using the Student's t-test. GraphPad Prism 6 (GraphPad Software) and SPSS (IMP SPSS statistics 23) were used to analyze the data. All values are expressed as mean ± SEM.

RESULTS

In this study, mice were divided into one of the three following groups: normal controls (ND, black), demyelination (CPZ, red), and remyelination ([CPZ] + 3ND, dark blue) (Fig. 1). After rapamycin was administered to half of the mice during demyelination (CPZ + Rapa, green) and examined following remyelination ([CPZ + Rapa] + 3ND, light blue), IHC was used to assess markers of demyelination, axonal integrity and inflammation. As demyelination of the CC in mice fed cuprizone diet is graded, following a caudal to rostral pathology (Steelman et al., 2012; Tagge et al., 2016), the CC of both rostral (0.85 to 0.95 mm from bregma) and caudal sections (−1.90 to −2.0 mm from bregma) were analyzed (Paxinos and Franklin, 2012).

Rapamycin Addition During Cuprizone Diet Did Not Influence Myelin Intensity

Cuprizone diet induces significant demyelination in the CC by 4.5 to 6 weeks (Matsushima and Morell, 2001; Crawford et al., 2009b). To assess the impact of rapamycin on myelination, brain sections were immunostained with myelin basic protein (MBP) and nuclei stain, 4′,6-diamidino-2-phenylindole (DAPI). Decreased MBP^+ immunoreactivity is shown in coronal brain montages in CPZ and CPZ + Rapa groups (Fig. 2Ai). After cuprizone administration, significant demyelination (CC area outlined in white boxes; Fig. 2Ai) was observed compared to the normal group, which is consistent with previous studies (Fig. 2Aii, iii, B, C). However, the addition of rapamycin with cuprizone diet did not result in a further decrease in MBP (Fig. 2A, B, C). Switching both CPZ and CPZ + Rapa groups back to normal diet for three weeks increased MBP^+ intensity (Fig. 2Aii,iii) for both [CPZ] + 3ND and [CPZ + Rapa] + 3ND (Fig. 2B, C). No significant difference in MBP^+ staining was observed between the remyelination groups (Fig. 2B, C). To further probe for effects of rapamycin administration on myelination, brain sections were also immunostained with myelin oligodendrocyte glycoprotein (MOG) (Fig. 3A), the last protein component expressed in the formation of myelin sheath which can therefore be evaluated as a more sensitive gauge for minimal changes in myelin protein (Lindner et al., 2008; Jahn et al., 2009; Crawford et al., 2009b). Decreased MOG^+ immunoreactivity was observed during demyelination compared to the ND control group, whereas an increase in MOG^+ intensity was seen three weeks after stopping the administration of cuprizone diet (Fig. 3B, C). Furthermore, the addition of rapamycin did not result in any further change in the levels of MOG during demyelination nor remyelination in caudal or rostral sections (Fig. 3B, C).

Rapamycin Increases Axon Damage During Cuprizone-Induced Demyelination

Three weeks of CPZ administration is sufficient to induce significant axonal dysfunction and damage (Crawford et al., 2009b). To assess the extent to which rapamycin affects axonal health, callosal white matter was probed for the non-phosphorylated heavy neurofilament epitope SMI-32, which is more abundant in damaged projection fibers (Sternberger and Sternberger, 1983; Trapp et al., 1998; Mangiardi et al., 2011). Elevated immunoreactivity for SMI-32 is shown in coronal brain montages of mice fed with cuprizone diet in the presence

and absence of rapamycin (Fig. 4Ai). A significant increase in SMI-32$^+$ intensity was observed in both rostral and caudal CC sections from non-rapamycin groups during acute demyelination compared to normal (Fig. 4Aiii, Av, B, C). Punctate, swollen callosal axons (Fig. 4Aii) were present in both demyelination groups where SMI-32$^+$ immunostaining shrouds the trace amounts of remaining visible MBP$^+$ signal (Fig. 4Aiv). Rapamycin-treated mice demonstrated regional differences in SMI-32$^+$ immunoreactivity during demyelination relative to the CPZ group as shown by an increase in rostral but not caudal sections (Fig. 4B, C). SMI-32$^+$ reactivity decreased in the caudal CC (Fig. 4B), yet increased in rostral CC sections (Fig. 4C), for both remyelination groups; [CPZ + Rapa] + 3ND and [CPZ] + 3ND; compared to demyelination. There was no significant difference in SMI-32$^+$ immunostaining between rapamycin and non-rapamycin remyelination groups.

Leukocyte Infiltration is Increased by Rapamycin During Cuprizone Diet

The pan-leukocyte marker cluster of differentiation (CD)45 was used to assess overall inflammation within the CC (Fig. 5A). Callosal CD45$^+$ immunoreactivity increased in the cuprizone group compared to the normal group in caudal, but not rostral sections (Fig. 5B, C). Concurrent rapamycin administration caused a dramatic increase in CD45$^+$ reactivity in rostral CC sections versus cuprizone alone (Fig. 5C) but caudal white matter showed comparable levels (Fig. 5B). CD45$^+$ reactivity declined during remyelination in the [CPZ] + 3ND group relative to CPZ in caudal sections (Fig. 5B). Additionally, CD45$^+$ reactivity decreased during remyelination in rapamycin-treated mice (Fig. 5B, C). Despite an overall decrease in CD45$^+$ signal during remyelination for both rapamycin and non-rapamycin groups, CD45$^+$ reactivity was significantly higher in [CPZ + Rapa] + 3ND rostral sections versus [CPZ] + 3ND (Fig. 5C). To distinguish microglia from macrophages and other leukocytes, immunostaining specific for the ionized calcium binding adaptor molecule-1 (Iba-1) was performed (Fig. 6A). Iba-1$^+$ reactivity was significantly higher in caudal sections during CPZ demyelination compared to the mice given normal diet (Fig. 6B), while rostral sections from mice treated with rapamycin showed elevated levels of Iba-1 compared to CPZ alone (Fig. 6C). During remyelination, Iba-1 levels were significantly reduced compared to demyelination except for the rostral rapamycin-treated group, which remained significantly elevated even after three weeks of normal diet (Fig. 6C).

Rapamycin Increases Astrogliosis During Remyelination

An increase in reactive astrocytes is observed in the cuprizone model (Bignami et al., 1972; Crawford et al., 2009b; Steelman et al., 2012). Elevated immunoreactivity for glial fibrillary acidic protein (GFAP) is shown in coronal brain montages from mice fed cuprizone (Fig. 7Ai). High magnification images show branched GFAP$^+$ cells (Fig. 7Ai and Aii white box insets). An overall increase in GFAP$^+$ immunoreactivity during demyelination in caudal CC sections (Fig. 7B) as well as in rostral CC sections (Fig. 7C) was observed. The addition of rapamycin during cuprizone-induced demyelination did not appear to alter GFAP$^+$ intensity beyond the effects observed with cuprizone diet alone (Fig. 7A, B, C). GFAP$^+$ reactive astrocytes decreased during remyelination in both caudal and rostral CC sections (Fig. 7B, C). However, in rostral CC sections, GFAP$^+$ intensity was elevated in the [CPZ + Rapa] + 3ND group compared to the [CPZ] + 3ND group (Fig. 7C). In contrast, GFAP + intensity

was not different in caudal CC sections between the [CPZ + Rapa] + 3ND group and the [CPZ] + 3ND group (Fig. 7B).

Rapamycin Addition Reduces Proliferating OPCs and Mature OLs

Spontaneous OPC proliferation and OPC differentiation occur during cuprizone diet. Because the mTOR pathway is important for the differentiation of OPCs into OLs, inhibiting this pathway with rapamycin should have a pronounced effect on OPCs and OLs within the CC. The effect of rapamycin during cuprizone diet on proliferating OPCs was determined by assessing the number of OLs labeled with the OL lineage-specific transcription factor (Olig2) co-stained with the prototypic cell cycle related nuclear protein Ki-67, which is expressed by proliferating cells (Fig. 8A). No significant change in the number of $Olig2^{+}Ki67^{+}$ OPCs was observed within the caudal or rostral CC sections (rostral not shown) in the CPZ group compared to normal controls (Fig. 8A, C). Surprisingly, proliferating OPC numbers in the mice receiving cuprizone with rapamycin were similar to the CPZ group during demyelination. While there was a trend toward an increase in proliferating OPCs during remyelination in [CPZ] + 3ND versus CPZ, it did not reach significant levels (Fig. 8C). Yet, the number of $Olig2^{+}Ki67^{+}$ cells was significantly reduced in the [CPZ + Rapa] + 3ND group compared to the [CPZ] + 3ND group (Fig. 8C).

The effect of rapamycin on mature OLs during cuprizone diet was determined by assessing the number of adenomatous polyposis coli ($CC1^{+}$) cells by IHC (Fig. 8B). During demyelination, a significant decrease in the number of $CC1^{+}$ cells was observed as compared to normal controls. No difference was observed between mice that received rapamycin and non-rapamycin cuprizone groups during demyelination (Fig. 8). The number of mature OLs significantly increased during remyelination [CPZ] + 3ND versus. CPZ (Fig. 8D). Additionally, the inclusion of rapamycin resulted in significantly lower numbers of $CC1^{+}$ cells during remyelination compared to the [CPZ] + 3ND group (Fig. 8D).

Rapamycin Reduces Callosal CAP Amplitude and Delays Conduction Velocity

Functional myelination was assessed by electrophysiological CAP recordings across rostral and caudal CC sections from acutely isolated brain slices (Fig. 9Ai). Typically, CAPs consist of two or more downward deflections referred to as N1 and N2. The first downward deflection, N1, represents the faster myelinated axons, while unmyelinated, or partially myelinated axons contribute to the second downward deflection, N2 (Crawford et al., 2009a). We observed a reduction in the myelinated component of the N1 peak amplitude for cuprizone-induced demyelination compared to ND in both rostral and caudal sections (Fig. 9B), with a further significant decrease in the myelinated component of the CAP for rostral rapamycin-treated groups (Fig. 9Bii). The amplitude of the second peak, N2, did not significantly change between any of the groups in caudal sections (Fig. 9Ci), although it was significantly increased in rostral sections for CPZ + Rapa compared to CPZ alone at the 4 mA stimulation intensity (Fig. 9Cii). Latency, an indicator of axonal conduction velocity and the types of axons contributing the CAP peaks, was also assessed. Distribution of latencies in demyelinating and remyelinating nerve fibers depend upon fundamental parameters of nerve fibers such as diameter, internodal length and extent of myelination. Interestingly, after

demyelination, N2 peak latency was significantly slower (~11%) in both rostral and caudal CC from the mice receiving rapamycin (Fig. 9D).

CAPs from caudal rapamycin and non-rapamycin remyelination sections showed no significant difference in the N1 nor the N2 peak amplitude (Fig. 10A, Bi, Ci). However, the N1 and N2 peak amplitudes were both increased in the rostral non-rapamycin remyelination group compared to the remyelination group that previously received rapamycin during cuprizone administration (Fig. 10Bii, Cii). Additionally, during remyelination, N2 peak latency in both caudal and rostral CC was significantly delayed (~21%) in the mice treated with rapamycin (Fig. 10D).

The present results are consistent with previous studies showing that by 4.5 weeks of cuprizone diet, demyelination of callosal axons is accompanied by damaged axons (Fig. 4). Thus, in the present study, the demyelinated and damaged callosal axons after 4.5 weeks of cuprizone diet may render the finite functional effects of rapamycin undetectable in caudal sections. Accordingly, an earlier time point of 1.5 weeks of cuprizone diet was used, where minimal damage of axons has been noted (Crawford et al., 2009b).

Rapamycin Administration for 1.5 Weeks of Cuprizone Reduces Microglial Reactivity But Does Not Affect CAPs or MOG Immunostaining

We administered rapamycin to animals fed cuprizone diet for 1.5 weeks to dissect the effects of rapamycin before the onset of global axon injury resulting from prolonged CPZ administration (Crawford et al., 2009b). MOG immunostaining (Fig. 11A) and Iba-1 immunostaining (Fig. 11B) were assessed in normal controls (ND, black), mice after 1.5 weeks of cuprizone diet (1.5CPZ, red) and mice that were fed cuprizone and received rapamycin injections for 1.5 weeks (1.5CPZ + Rapa, green). Myelination examined by MOG showed reduced levels during demyelination but no significant difference between rapamycin and non-rapamycin groups (Fig. 11Ci), and the population of activated microglia increased for both 1.5-week demyelination groups, although to a lesser extent when rapamycin injections were combined with 1.5 weeks of CPZ (Fig. 11Cii). CAPs were also recorded (Fig. 11D), exhibiting no significant change in the N1 nor N2 peak amplitude (Fig. 11E), or latency (Fig. 11F) in any of the groups at the 1.5-week time point.

DISCUSSION

The cuprizone diet mouse model is widely used to study the mechanisms of demyelination and remyelination as well as neuroprotective and regenerative agents (Plant et al., 2007; Zhang et al., 2012; Bai et al., 2016). However, studies employing the cuprizone model may be confounded by incidences of endogenous myelin recovery which may mask small but significant therapeutic effects during remyelination. Within the CC, OPCs reach a proliferative peak after ~4–5 weeks of cuprizone diet in an ongoing attempt to replenish OLs, which then undergo apoptosis in the presence of cuprizone (Matsushima and Morell, 2001). Yet a subpopulation of newly formed OLs survive and produce myelin that ensheathe axons (Islam et al., 2009).

Within the last decade, researchers have started administering mTOR inhibitors (rapamycin and analogues) during cuprizone diet in an effort to inhibit OPC proliferation and achieve complete axonal demyelination (Narayanan et al., 2009; Hu et al., 2011; Sachs et al., 2014). However, the effects of rapamycin within this model have not been well characterized (Gudi et al., 2014). While our laboratory has investigated the effects of cuprizone-induced demyelination at multiple time points (from 1.5 to 12 weeks) these studies did not supplement the model with rapamycin (Crawford et al., 2009a,b; Lapato et al., 2017). Compelled by the prospect of achieving more complete demyelination within our model, in a recent evaluation of a therapeutic agent, we included rapamycin as advised by the current literature (Narayanan et al., 2009; Sachs et al., 2014; Bai et al., 2016). However, unlike previous reports, our results failed to find differences in the extent of demyelination despite using the same concentration of rapamycin. This prompted the current study in which we sought to characterize some of the effects of rapamycin treatment with cuprizone administration.

During demyelination, rapamycin treatment did not significantly change OPC/OL numbers, consistent with published results (Sachs et al., 2014). In addition, rapamycin treatment showed no difference in the extent of demyelination as observed by MBP and MOG immunostaining. During the formation of the myelin sheath, MBP occupies an integral location at an earlier time point and is later surrounded by MOG (Jahn et al., 2009). Therefore, it is useful to examine both MBP and MOG immunostaining for a thorough assessment of the alterations in myelination that could occur at varying rates or within different structural components of the myelin sheath. Others have reported that rapamycin treatment during 6 weeks of 0.3% cuprizone diet resulted in a significant decrease in MOG immunostaining (Sachs et al., 2014), although we found that 0.2% cuprizone and rapamycin together did not induce any further loss of MBP or MOG immunostaining than cuprizone alone for 4.5 weeks.

Our previous studies have shown that administration of cuprizone diet for more than three weeks increases axonopathy (Crawford et al., 2009a, b; Moore et al., 2014). To assess axon integrity, we performed IHC with SMI-32, a neuronal marker present in low levels in axons. When axonal transport becomes impaired during demyelination, SMI-32 accumulates in the CC axons and has been used as a marker for axon damage (Sternberger and Sternberger, 1983; Trapp et al., 1998; Mangiardi et al., 2011). SMI-32^{+} intensity increased in demyelination groups compared to normal. A further increase in SMI-32 was observed with rapamycin treatment, similar to the results reported by Sachs and colleagues with rapamycin treatment for SMI-32 and amyloid precursor protein (APP) (Sachs et al., 2014). Typically, during cuprizone diet, there is an increase in infiltrating leukocytes and reactive astrogliosis, which was also observed in this study. With the addition of rapamycin during demyelination, an increase in Iba-1^{+} microglia, and CD45^{+} infiltrating leukocytes was observed, but GFAP^{+} intensity was unaltered. Sachs and colleagues observed a similar increase in Iba-1^{+} immunostaining yet, unlike our observation, an increase in GFAP^{+} immunostaining in the CPZ + Rapa group relative to the CPZ group (Sachs et al., 2014). This could be due to experimental paradigm differences including the concentration of cuprizone diet (0.3% CPZ used in Sachs et al., 2014 study versus 0.2% CPZ used in our study) and/or the duration of cuprizone diet (6 weeks in Sachs' study versus 4.5 weeks of CPZ diet in our study).

Additionally, as astrocytes and microglia have an integral role in a plethora of OPC and OL processes the addition of rapamycin to this model may have additional confounding effects on the interpretation of these studies by altering glia physiology.

The electrophysiological effects in caudal sections of combining rapamycin administration with cuprizone diet were found to be consistent with the results obtained from IHC. Demyelination was severe after 4.5 weeks of cuprizone and decreased the N1 component of the CAP to insignificant levels so that no further effect of rapamycin on myelination could be observed. However, alongside increased axon damage observed with SMI-32 IHC data, rapamycin groups revealed an increase in both rostral and caudal CC N2 latency, indicating potential axon damage. We also report a difference in conduction of myelinated axons from rostral sections, during both demyelination and remyelination. The decrease in N1 for rostral rapamycin-treated groups during demyelination could have triggered a compensatory response via an increase in the number of the slower unmyelinated axons contributing to the N2 component of the CAP, although N2 latency was still increased in these axons. The slight increase in the N2 component of the CAP observed at the highest stimulation intensity in rapamycin-treated groups during demyelination is not seen during remyelination. Instead, rapamycin-treated groups exhibited an N2 CAP component with a dramatically lower amplitude compared to the non-rapamycin-treated remyelination group. This functional impairment is consistent with an increased N2 component latency, which is more dramatic than the increase seen in rapamycin-treated groups during demyelination. Thus, rapamycin treatment appears to exert negative effects on conduction in a manner which seems to compile over time, in some cases becoming more severe (loss of N2 CAP amplitude), even after the rapamycin administration period has ended. In particular, the notable differences between rapamycin and non-rapamycin groups reported following remyelination points to a previously unknown, long-lasting effect of rapamycin that is resilient even to three weeks of normal diet in the absence of any demyelinating agent.

Furthermore, mature OLs immunopositive for CC1 in the CC were decreased following demyelination, compared to normal, with no significant difference between CPZ and CPZ + Rapa. However, in mice treated with rapamycin during cuprizone, $CC1^+$ OL numbers failed to reach the high levels restored in non-rapamycin groups during normal diet remyelination. These findings contradict previous studies in which the CPZ + Rapa group was found to have fewer mature glutathione S-transferase $(GST)\pi^+$ and $CC1^+$ OLs after six weeks of 0.3% cuprizone plus rapamycin administration (Narayanan et al., 2009; Sachs et al., 2014). Additionally, after one and seven weeks of remyelination (three week normal diet time-point not evaluated) mature OL counts recovered, even in groups previously treated with rapamycin (Sachs et al., 2014).

Unlike mature OLs, proliferating OPCs double labeled with Olig2 and Ki67 were unchanged during demyelination, compared to normal. Other studies have shown that after six weeks demyelination there is an increase in OPCs labeled with nerve glial antigen 2 (NG2), a proteoglycan marker of a cycling progenitor population capable of producing OLs as well as astrocytes (Dawson et al., 2000; Polito and Reynolds, 2005). A significant increase in $NG2^+$ OPCs was also reported for rapamycin-treated groups, compared to non-rapamycin 0.3% cuprizone groups. After three weeks of remyelination, we observed an increase only in

proliferating OPCs from non-rapamycin groups. However, following seven weeks of remyelination, it has been shown that OPC levels have decreased compared to demyelination (Sachs et al., 2014). The increase in proliferating OPCs counted during remyelination is in contrast to the low proliferating OPC counts previously reported (Sachs et al., 2014). The higher ratio of OPCs to mature OLs in our study compared to those previously published could be explained in part by the loss of functional conductivity due to increased axonal damage that could be thereby preventing the progression of OPCs to later stages in which they differentiate to form mature OLs.

To better understand the inhibitory effect of rapamycin on callosal conduction occurring in the absence of any broad changes in CC myelination, we questioned whether a comparable outcome could be induced by a shorter 1.5-week demyelination time point. Cuprizone demyelination for 1.5 weeks has been previously reported by our laboratory to minimally reduce myelinated CAP peak amplitude and MOG immunoreactivity while escaping the extensive axon damage manifested by three or more weeks (Crawford et al., 2009b). It then follows that incorporating rapamycin injections to the 1.5-week cuprizone demyelination paradigm would reveal functional effects primarily attributable to the presence of rapamycin, as opposed to those of cuprizone-induced axonal pathology. CAPs recorded in slices from 1.5 week demyelination groups showed only minor N1 amplitude differences that did not reach significance in comparison to the normal diet control group, although a more significant reduction in N1 amplitude has been shown previously (Crawford et al., 2009b). Improvements made over time to our electrophysiology slicing protocol could potentially have contributed to the attainment of healthier slices from 1.5-week CPZ mice that enabled recordings to be less distinguishable from control slices. Rapamycin as a supplement to cuprizone diet for 1.5 weeks did not induce any significant electrophysiological changes indicative of negative effects on axon health, consistent with a lack of axon damage reported from immunostaining with SMI-32 and APP, (Crawford et al., 2009b). Demyelination at 1.5 weeks was instead evidenced by a decrease in MOG immunostaining regardless of the presence of rapamycin and associated with an increase in callosal microglial activation and accumulation that was more remarkable in the 1.5 week CPZ group than in the 1.5 week CPZ + Rapa group. The decrease in microglial activation in the rapamycin-treated group is consistent with previously published data illustrating that rapamycin treatment can reduce microglial activation (Tateda et al., 2017), however decreasing activated microglia in this model could be leading to slower clearance of debris and dysfunctional cells leading to increased axonal damage. The lack of different myelination levels observed between rapamycin and non-rapamycin groups at 1.5 weeks of demyelination supports the conclusion that rapamycin does not, in fact, measurably contribute to comprehensive demyelination in a way that would be advantageous when combined with cuprizone. While rapamycin did reduce OPCs and mature OLs at longer time points, the effects of inhibiting the mTOR pathway with rapamycin is not limited to OLs but also affects astrocytes, microglia, and neurons, thereby potentially confounding studies examining demyelination and remyelination mechanisms as well as therapeutic out-comes. Results provided in the present study question the use of rapamycin during cuprizone administration. No further decrease in myelin was observed during cuprizone diet in the presence of rapamycin. Rather, the neuropathological effects of including rapamycin during cuprizone administration included

increased axonal damage, leukocyte infiltration, and reactive gliosis within the CC. Additionally, the myelinated axon component of the CAP recording showed decreased amplitude and the unmyelinated component showed increased latency as compared to non-rapamycin treated cuprizone animals.

These negative effects of the addition of rapamycin to the cuprizone model have the capacity to significantly confound remyelination studies to such an extent that it is perhaps not worth the potential benefit of incorporating an mTOR inhibitor to achieve more complete demyelination.

ACKNOWLEDGMENTS

This work was supported by research funded by National Institutes of Health Grant R01 NS081141-01A1 and National Multiple Sclerosis Society Grant RG 4853A3/2 to STW. We would like to thank all the laboratory members for critical reading of the manuscript.

Abbreviations:

CAP	compound action potential
CC	corpus callosum
CPZ	cuprizone
MS	multiple sclerosis
mTOR	mammalian/mechanistic target of rapamycin
OL	oligodendrocyte
OPC	oligodendrocyte progenitor cell
PI3K/Akt	phosphatidylinositol kinase 3/Protein kinase B
Rapa	rapamycin

REFERENCES

Bai CB, Sun S, Roholt A, Benson E, Edberg D, Medicetty S, Dutta R, Kidd G, et al. (2016) A mouse model for testing remyelinating therapies. Exp Neurol 283:330–340. [PubMed: 27384502]

Baxter AG. (2007) The origin and application of experimental autoimmune encephalomyelitis. Nat Rev Immunol 7:904–912. [PubMed: 17917672]

Bénardais K, Kotsiari A, Skuljec J, Koutsoudaki PN, Gudi V, Singh V, Vulinović F, Skripuletz T, et al. (2013) Cuprizone [bis(cyclohexylidene-hydrazide)] is selectively toxic for mature oligodendrocytes. Neurotox Res 24:244–250. [PubMed: 23392957]

Bercury KK, Dai J, Sachs HH, Ahrendsen JT, Wood TL, Macklin WB. (2014) Conditional ablation of raptor or rictor has differential impact on oligodendrocyte differentiation and CNS myelination. J Neurosci 34:4466–4480. [PubMed: 24671993]

Bignami A, Eng LF, Dahl D, Uyeda CT. (1972) Localization of the glial fibrillary acidic protein in astrocytes by immunofluorescence. Brain Res 43:429–435. [PubMed: 4559710]

Blakemore WF, Franklin RJM. (2008) Remyelination in experimental models of toxin-induced demyelination In: & Rodriguez M, editor. Advances in multiple Sclerosis and Experimental Demyelinating Diseases. Berlin, Heidelberg: Springer Berlin Heidelberg p. 193–212.

Crawford DK, Mangiardi M, Tiwari-Woodruff SK. (2009) Assaying the functional effects of demyelination and remyelination: revisiting field potential recordings. J Neurosci Methods 182:25–33. [PubMed: 19481113]

Crawford DK, Mangiardi M, Xia X, Lopez-Valdes HE, Tiwari-Woodruff SK. (2009) Functional recovery of callosal axons following demyelination: a critical window. Neuroscience 164:1407–1421. [PubMed: 19800949]

Dai J, Bercury KK, Macklin WB. (2014) Interaction of mTOR and Erk1/2 signaling to regulate oligodendrocyte differentiation. Glia 62:2096–2109. [PubMed: 25060812]

Dawson MR, Levine JM, Reynolds R. (2000) NG2-expressing cells in the central nervous system: are they oligodendroglial progenitors? J Neurosci Res 61:471–479. [PubMed: 10956416]

Denic A, Johnson AJ, Bieber AJ, Warrington AE, Rodriguez M, Pirko I. (2011) The relevance of animal models in multiple sclerosis research. Pathophysiology 18:21–29. [PubMed: 20537877]

Guardiola-Diaz HM, Ishii A, Bansal R. (2012) Erk1/2 MAPK and mTOR signaling sequentially regulates progression through distinct stages of oligodendrocyte differentiation. Glia 60:476–486. [PubMed: 22144101]

Gudi V, Gingele S, Skripuletz T, Stangel M. (2014) Glial response during cuprizone-induced de- and remyelination in the CNS: lessons learned. Front Cell Neurosci 8:73. [PubMed: 24659953]

Hasselmann JPC, Karim H, Khalaj AJ, Ghosh S, Tiwari-Woodruff SK. (2017) Consistent induction of chronic experimental autoimmune encephalomyelitis in C57BL/6 mice for the longitudinal study of pathology and repair. J Neurosci Methods 284:71–84. [PubMed: 28396177]

Hu Y, Lee X, Ji B, Guckian K, Apicco D, Pepinsky RB, Miller RH, Mi S. (2011) Sphingosine 1-phosphate receptor modulator fingolimod (FTY720) does not promote remyelination in vivo. Mol Cell Neurosci 48:72–81. [PubMed: 21740973]

Islam MS, Tatsumi K, Okuda H, Shiosaka S, Wanaka A. (2009) Olig2-expressing progenitor cells preferentially differentiate into oligodendrocytes in cuprizone-induced demyelinated lesions. Neurochem Int 54:192–198. [PubMed: 19070638]

Jahn O, Tenzer S, Werner HB. (2009) Myelin proteomics: molecular anatomy of an insulating sheath. Mol Neurobiol 40:55–72. [PubMed: 19452287]

Karim H, Kim SH, Lapato AS, Yasui N, Katzenellenbogen JA, Tiwari-Woodruff SK. (2018) Increase in chemokine CXCL1 by ERbeta ligand treatment is a key mediator in promoting axon myelination. Proc Natl Acad Sci U S A 115(24):6291–6296. [PubMed: 29844175]

Lapato AS, Szu JI, Hasselmann JPC, Khalaj AJ, Binder DK, Tiwari-Woodruff SK. (2017) Chronic demyelination-induced seizures. Neuroscience 346:409–422. [PubMed: 28153692]

Lauderdale K, Murphy T, Tung T, Davila D, Binder DK, Fiacco TA. (2015) Osmotic edema rapidly increases neuronal excitability through activation of NMDA receptor-dependent slow inward currents in juvenile and adult Hippocampus. ASN Neuro 7.

Lebrun-Julien F, Bachmann L, Norrmen C, Trotzmuller M, Kofeler H, Ruegg MA, Hall MN, Suter U. (2014) Balanced mTORC1 activity in oligodendrocytes is required for accurate CNS myelination. J Neurosci 34:8432–8448. [PubMed: 24948799]

Lindner M, Heine S, Haastert K, Garde N, Fokuhl J, Linsmeier F, Grothe C, Baumgärtner W, et al. (2008) Sequential myelin protein expression during remyelination reveals fast and efficient repair after central nervous system demyelination. Neuropathol Appl Neurobiol 34:105–114. [PubMed: 17961136]

Lipton JO, Sahin M. (2014) The neurology of mTOR. Neuron 84:275–291. [PubMed: 25374355]

Mangiardi M, Crawford DK, Xia X, Du S, Simon-Freeman R, Voskuhl RR, Tiwari-Woodruff SK. (2011) An animal model of cortical and callosal pathology in multiple sclerosis. Brain Pathol 21:263–278. [PubMed: 21029240]

Matsushima GK, Morell P. (2001) The neurotoxicant, cuprizone, as a model to study demyelination and remyelination in the central nervous system. Brain Pathol 11:107–116. [PubMed: 11145196]

McCarthy DP, Richards MH, Miller SD. (2012) Mouse models of multiple sclerosis: experimental autoimmune encephalomyelitis and theiler's virus-induced demyelinating disease. Methods Mol Biol 900:381–401. [PubMed: 22933080]

Moore SM, Khalaj AJ, Kumar S, Winchester Z, Yoon J, Yoo T, Martinez-Torres L, Yasui N, et al. (2014) Multiple functional therapeutic effects of the estrogen receptor beta agonist indazole-cl in a

mouse model of multiple sclerosis. Proc Natl Acad Sci U S A 111:18061–18066. [PubMed: 25453074]

Narayanan SP, Flores AI, Wang F, Macklin WB. (2009) Akt signals through the mammalian target of rapamycin pathway to regulate CNS myelination. J Neurosci 29:6860–6870. [PubMed: 19474313]

Patel R, Moore S, Crawford DK, Hannsun G, Sasidhar MV, Tan K, Molaie D, Tiwari-Woodruff SK. (2013) Attenuation of corpus callosum axon myelination and remyelination in the absence of circulating sex hormones. Brain Pathol 23:462–475. [PubMed: 23311751]

Paxinos G, Franklin K. (2012) Paxinos and Franklin's the mouse brain in stereotaxic coordinates. Academic Press, 2012.

Plant SR, Iocca HA, Wang Y, Thrash JC, O'Connor BP, Arnett HA, Fu YX, Carson MJ, et al. (2007) Lymphotoxin beta receptor (Lt betaR): dual roles in demyelination and remyelination and successful therapeutic intervention using Lt betaR-Ig protein. J Neurosci 27:7429–7437. [PubMed: 17626203]

Polito A, Reynolds R. (2005) NG2-expressing cells as oligodendrocyte progenitors in the normal and demyelinated adult central nervous system. J Anat 207:707–716. [PubMed: 16367798]

Ransohoff RM. (2012) Animal models of multiple sclerosis: the good, the bad and the bottom line. Nat Neurosci 15:1074–1077. [PubMed: 22837037]

Sachs HH, Bercury KK, Popescu DC, Narayanan SP, Macklin WB. (2014) A new model of cuprizone-mediated demyelination/remyelination. ASN Neuro 6.

Steelman AJ, Thompson JP, Li J. (2012) Demyelination and remyelination in anatomically distinct regions of the corpus callosum following cuprizone intoxication. Neurosci Res 72:32–42. [PubMed: 22015947]

Sternberger LA, Sternberger NH. (1983) Monoclonal antibodies distinguish phosphorylated and nonphosphorylated forms of neurofilaments in situ. Proc Natl Acad Sci U S A 80:6126–6130. [PubMed: 6577472]

Sternberger NH, McFarlin DE, Traugott U, Raine CS. (1984) Myelin basic protein and myelin-associated glycoprotein in chronic, relapsing experimental allergic encephalomyelitis. J Neuroimmunol 6:217–229. [PubMed: 6203931]

Tagge I, O'Connor A, Chaudhary P, Pollaro J, Berlow Y, Chalupsky M, Bourdette D, Woltjer R, Johnson M, Rooney W. (2016) Spatio-temporal patterns of demyelination and remyelination in the cuprizone mouse model. PLoS One 11 e0152480. [PubMed: 27054832]

Tateda S, Kanno H, Ozawa H, Sekiguchi A, Yahata K, Yamaya S, Itoi E. (2017) Rapamycin suppresses microglial activation and reduces the development of neuropathic pain after spinal cord injury. J Orthop Res 35:93–103. [PubMed: 27279283]

Trapp BD, Peterson J, Ransohoff RM, Rudick R, Mork S, Bo L. (1998) Axonal transection in the lesions of multiple sclerosis. N Engl J Med 338:278–285. [PubMed: 9445407]

Tyler WA, Gangoli N, Gokina P, Kim HA, Covey M, Levison SW, Wood TL. (2009) Activation of the mammalian target of rapamycin (mTOR) is essential for oligodendrocyte differentiation. J Neurosci 29:6367–6378. [PubMed: 19439614]

Wahl SE, McLane LE, Bercury KK, Macklin WB, Wood TL. (2014) Mammalian target of rapamycin promotes oligodendrocyte differentiation, initiation and extent of CNS myelination. J Neurosci 34:4453–4465. [PubMed: 24671992]

Wekerle H, Kojima K, Lannes-Vieira J, Lassmann H, Linington C. (1994) Animal models. Ann Neurol 36:S47–S53 [Suppl]. [PubMed: 7517126]

Wood TL, Bercury KK, Cifelli SE, Mursch LE, Min J, Dai J, Macklin WB. (2013) mTOR: a link from the extracellular milieu to transcriptional regulation of oligodendrocyte development. ASN Neuro 5e00108.

Zhang Y, Zhang H, Wang L, Jiang W, Xu H, Xiao L, Bi X, Wang J, et al. (2012) Quetiapine enhances oligodendrocyte regeneration and myelin repair after cuprizone-induced demyelination. Schizophr Res 138:8-17. [PubMed: 22555017]

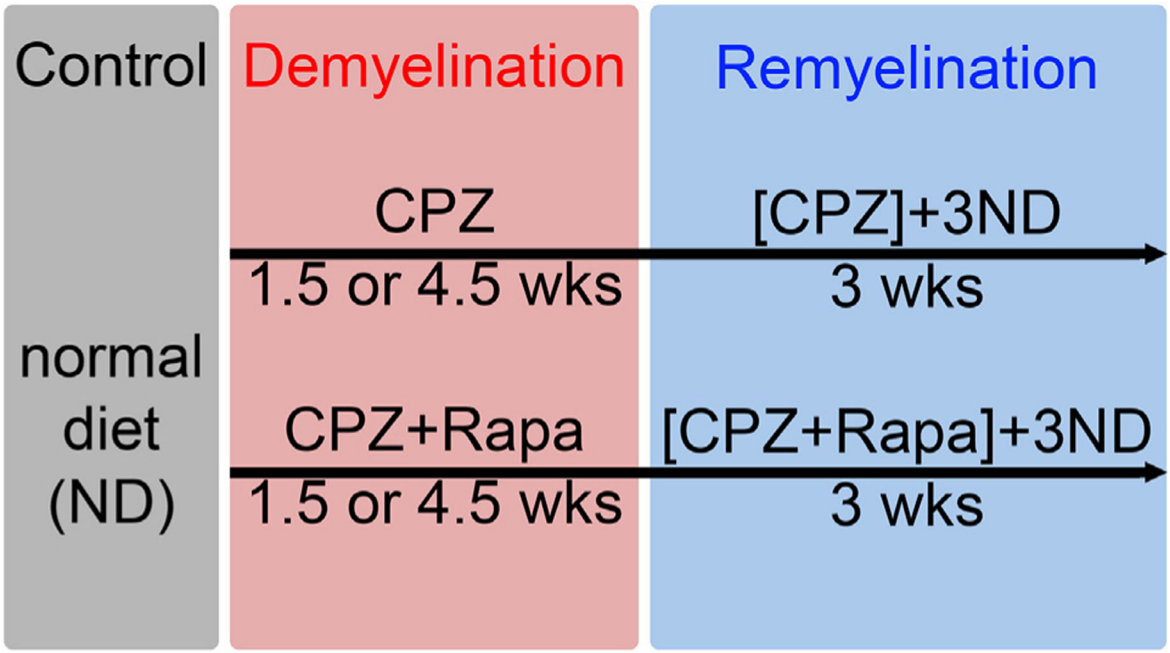

Fig. 1.

Eight-week-old male C57BL/6 mice were divided into control, demyelination, or remyelination groups. The control group was fed normal diet only (ND). Demyelination groups were fed cuprizone diet (CPZ) for either 1.5 or 4.5 weeks, with or without intraperitoneal rapamycin (Rapa) injections (10 mg/kg). Remyelination groups were fed CPZ diet for 4.5 weeks +/− Rapa injections and then switched to ND for 3 subsequent weeks. Tissue was processed for IHC and CAP recordings.

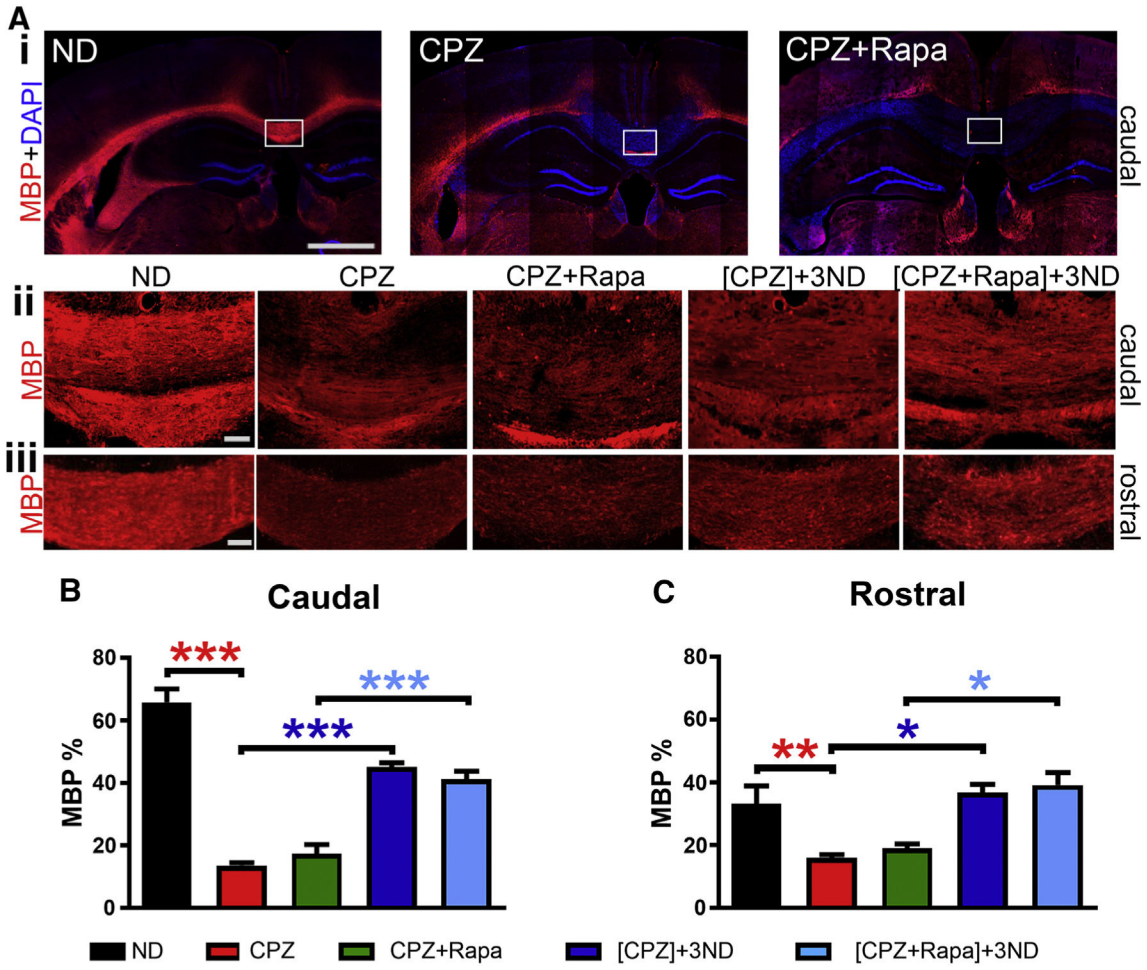

Fig. 2.

Rapamycin does not change myelin basic protein (MBP) immunostaining in the CC. (A) (i) Representative 10× magnification montages of coronal brain sections immunostained for MBP and nuclei (DAPI) from ND, CPZ and CPZ + Rapa groups (scale bar: 1 mm). White boxes indicate the region of the CC quantified. Representative 10× images of MBP immunostaining in caudal (ii) and rostral (iii) CC sections from all groups. (B/C) MBP staining intensity decreased during demyelination compared to ND and recovered during remyelination. No difference was observed between Rapa and non-Rapa groups, nor between rostral and caudal CC sections. All scale bars: 100 μm, unless otherwise specified.

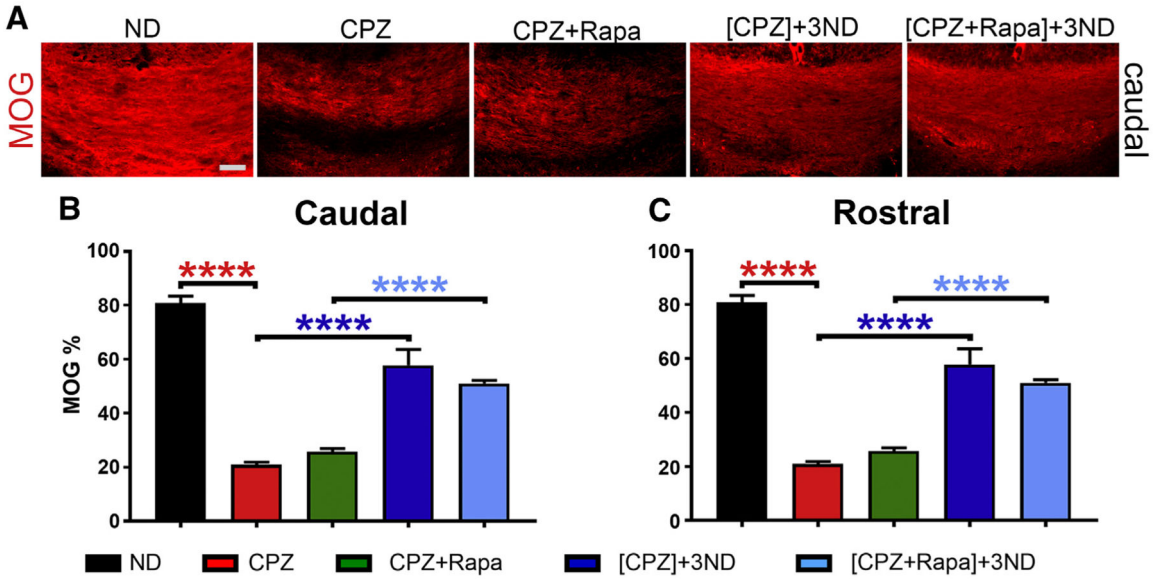

Fig. 3.

Rapamycin does not change myelin oligodendrocyte glycoprotein (MOG) immunostaining in the CC. (A) Representative 10× coronal brain section images of MOG immunostaining in the CC from ND, 4.5CPZ, 4.5CPZ + Rapa, [4.5CPZ] + 3ND, and [4.5CPZ + Rapa] + 3ND groups. (B/C) MOG staining intensity decreased during demyelination compared to ND and recovered during remyelination. No difference was observed between Rapa and non-Rapa groups, nor between rostral and caudal CC sections. Scale bar: 100 μm.

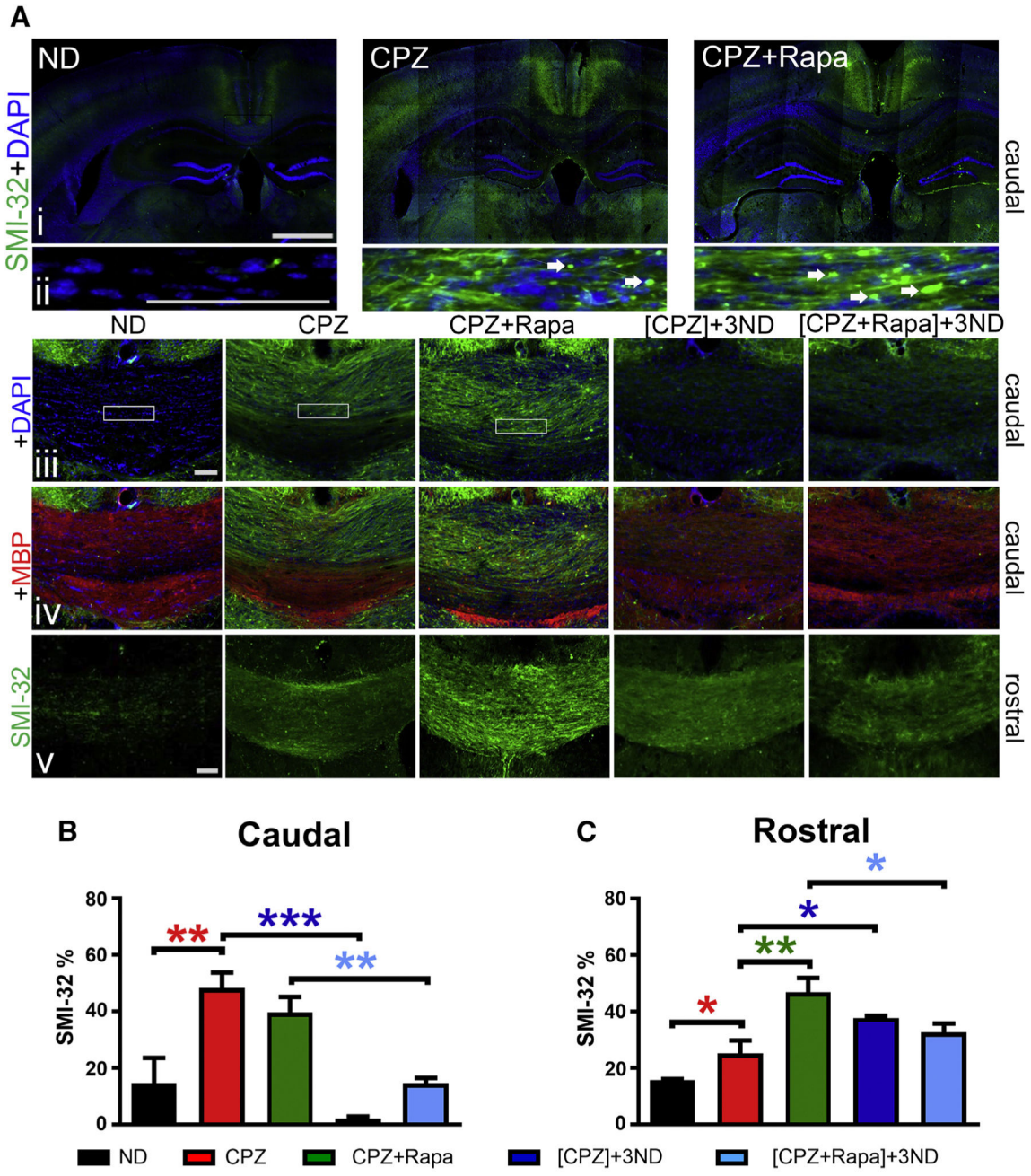

Fig. 4.

Rapamycin increases SMI-32 immunostaining in the CC. (A) (i) Representative 10× magnification montages of coronal brain sections immunostained for non-phosphorylated neurofilament SMI-32 and nuclei (DAPI) from ND, CPZ, and CPZ + Rapa groups (scale bar: 1 mm). (ii) High magnification images (scale bar: 100 μm) of SMI-32 and DAPI in CC fibers from groups in (i), including white arrows to identify the appearance of axonal blebbing. Representative 10× images of SMI-32 and DAPI (iii) and merged with MBP (iv) in caudal CC sections from all groups. (v) Representative 10× images of SMI-32 in rostral CC sections from all groups. White boxes indicate the region of CC depicted in (ii). (B/C)

SMI-32 staining intensity increased in CPZ compared to ND and was significantly higher in rostral CPZ + Rapa compared to CPZ. SMI-32 intensity decreased during remyelination compared to CPZ, both with and without Rapa (except that SMI-32 intensity increased in the rostral remyelination group compared to CPZ). No difference was observed during [CPZ + Rapa] + 3ND, compared to [CPZ] + 3ND. All scale bars: 100 μm, unless otherwise specified.

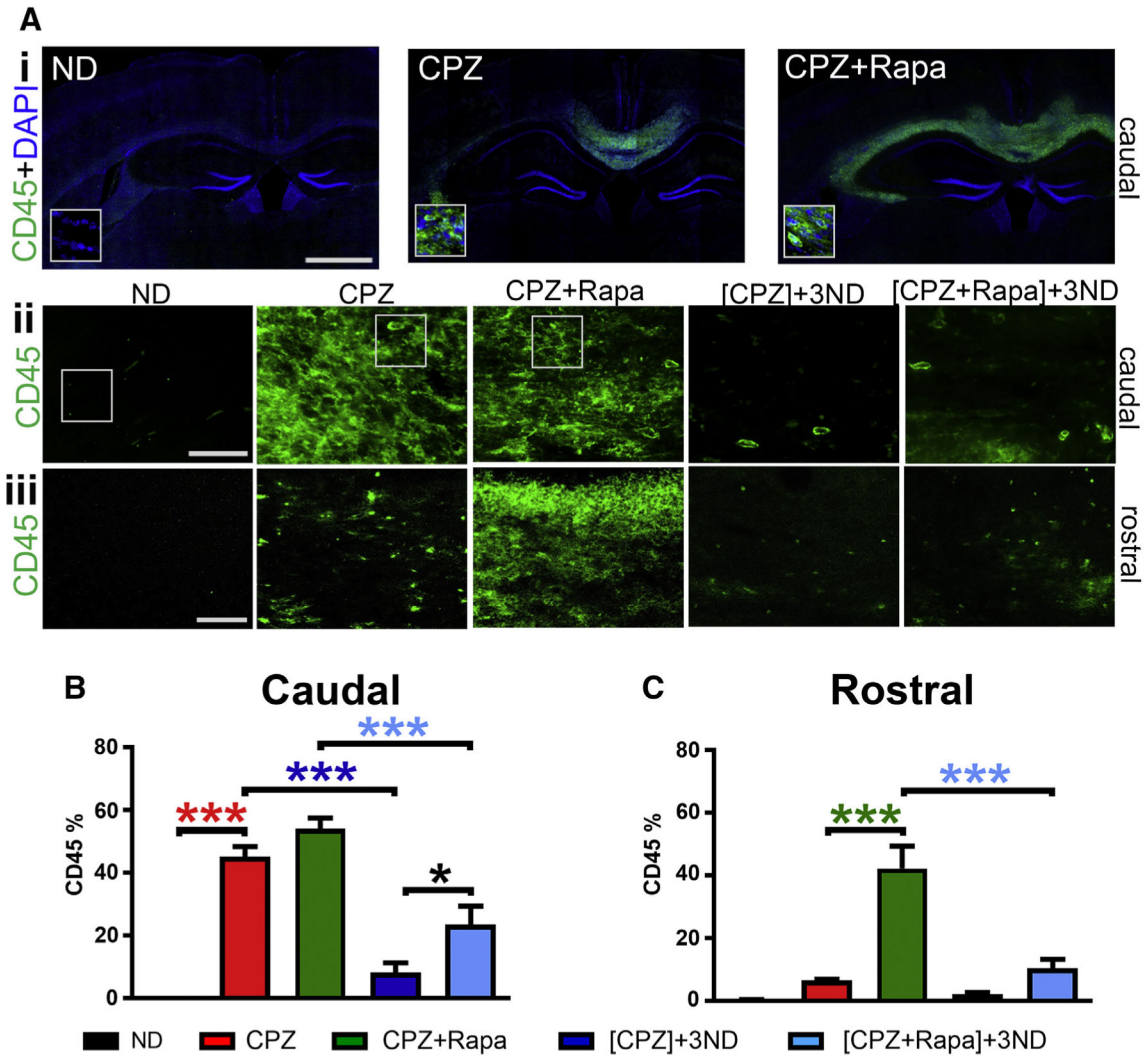

Fig. 5.

Rapamycin increases leukocyte common antigen expression during demyelination. (A) (i) Representative 10× magnification montages of coronal brain sections immunostained for common leukocyte antigen cluster of differentiation (CD) microglia/macrophage marker (CD45) and nuclei (DAPI)from ND, CPZ, and CPZ + Rapa groups (scale bar: 1 mm). White boxes highlight the absence of CD45+ cells in high magnification CC images from ND relative to multiple CD45+ leukocytes co-labeled with DAPI in both CPZ and CPZ + Rapa. Representative 20× images of CD45 in caudal (ii) and rostral (iii) CC sections from all groups. (B/C) Levels of CD45 were increased during CPZ compared to ND in caudal sections but not in rostral sections, however CD45 levels were significantly higher for CPZ + Rapa in both rostral and caudal sections. Levels of CD45 were decreased during remyelination compared to demyelination in both with and without Rapa mice. All scale bars: 100 μm, unless otherwise specified.

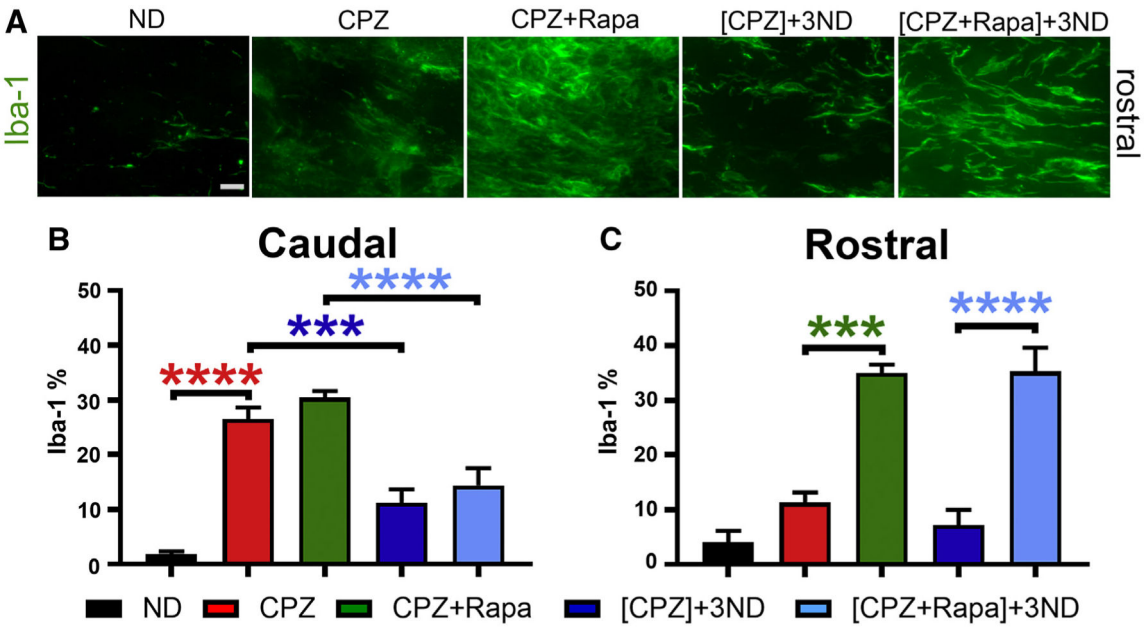

Fig. 6.

Rapamycin increases ionized calcium binding adaptor molecule-1 (Iba-1) expression during demyelination and remyelination. (A) Representative 40× coronal brain section images of Iba-1 immunostaining in the CC from ND, 4.5CPZ, 4.5CPZ + Rapa, [4.5CPZ] + 3ND, and [4.5CPZ + Rapa] + 3ND groups. (B/C) Iba-1 staining intensity increased during demyelination, to a significantly greater degree in caudal brain sections. Rapamycin presence during cuprizone diet increased levels of Iba-1 intensity in CC of both caudal and rostral brain slices. During remyelination, Iba-1 staining was greatly reduced except for the rostral remyelination group previously treated with CPZ + Rapa, which exhibited Iba-1 levels that remained elevated after 3 weeks of normal diet. Scale bar: 10 μm.

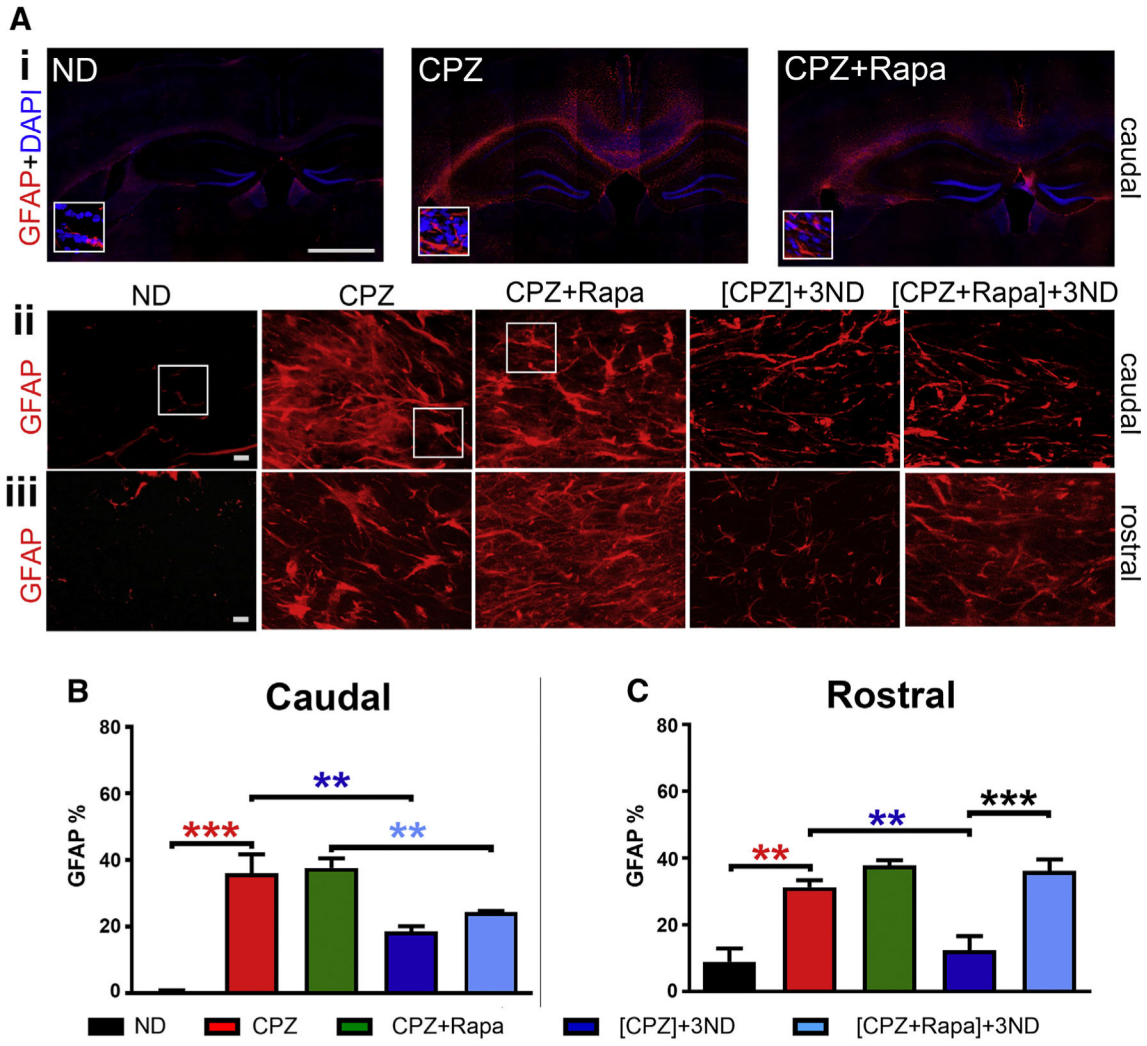

Fig. 7.

Rapamycin increases GFAP reactivity during remyelination. (A) (i) Representative 10× magnification montages of coronal brain sections immunostained for glial fibrillary acidic protein (GFAP) and nuclei (DAPI) from ND, CPZ, and CPZ + Rapa groups (scale bar: 1 mm). White boxes depict individual GFAP+ astrocytes co-labeled with DAPI in high magnification CC images from ND, CPZ, and CPZ + Rapa groups. Representative 20× images of GFAP in caudal (ii) and rostral (iii) CC sections from all groups. (B/C) Although levels of GFAP intensity were increased during CPZ compared to ND, no difference was observed in GFAP immunostaining between CPZ and CPZ + Rapa. Rapa did, however, result in significantly higher levels for [CPZ + Rapa] + 3ND compared to [CPZ] + 3ND in rostral sections. All scale bars: 10 μm, unless otherwise specified.

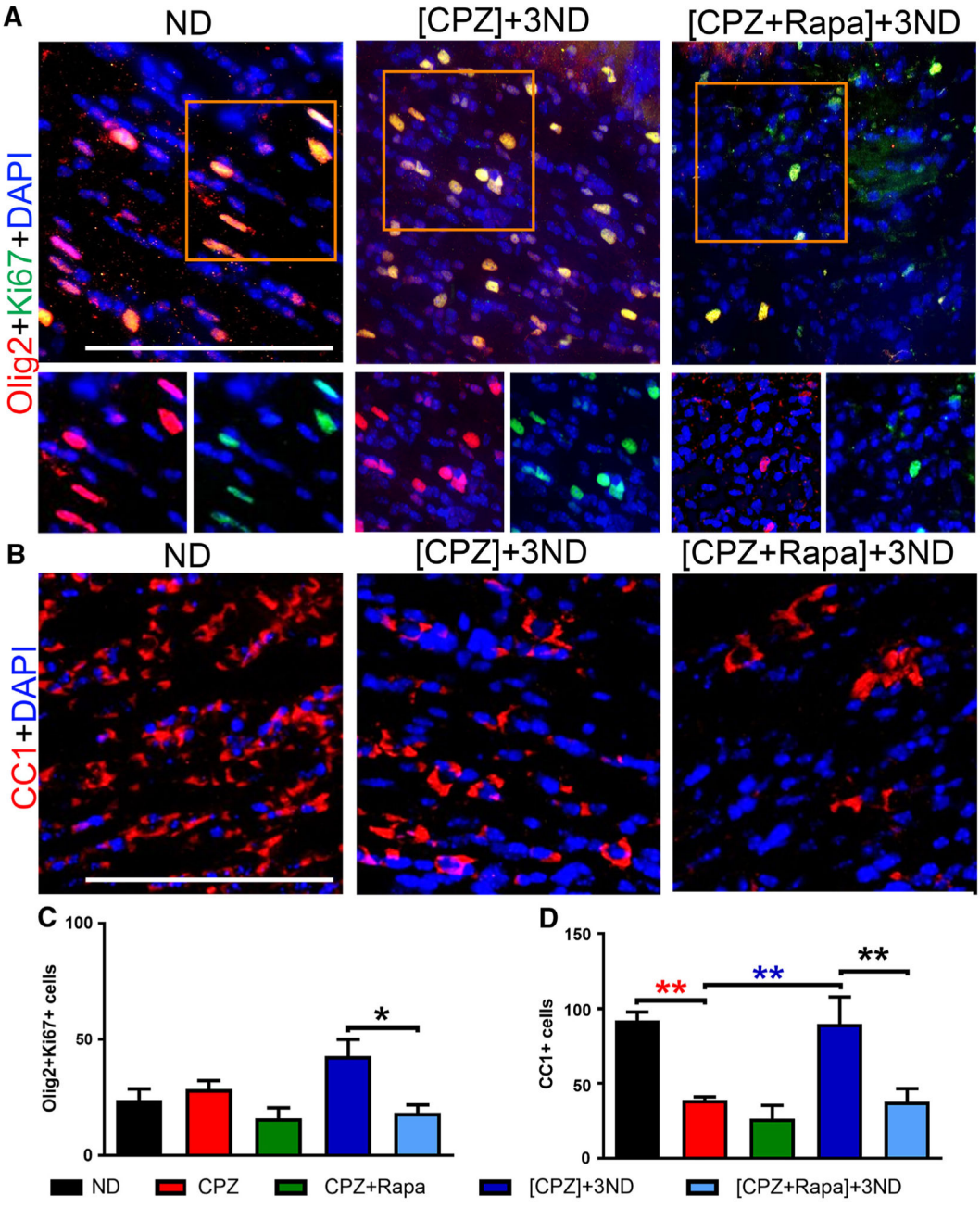

Fig. 8.

Rapamycin prevents the recovery of proliferating OPCs and mature OLs during remyelination in caudal CC sections. (A) Representative 40× magnification images of transcription factor Olig2, proliferation marker Ki67, and nuclei (DAPI) in caudal CC sections from ND, [CPZ] + 3ND, and [CPZ + Rapa] + 3ND. Orange dotted boxes in merged images were split to show the Olig2 and Ki67 channels separately with DAPI below each image. (B) Representative 40× magnification images of mature OL marker CC1 and nuclei (DAPI) in caudal CC sections from ND, [CPZ] + 3ND, and [CPZ + Rapa] + 3ND. (C/D) Cell counts were obtained from two 40× images of the center CC. Numbers of proliferating OPCs (C), identified by co-labeling with Olig2 and Ki67, as well as CC1 + OLs (D), were

unchanged between ND and CPZ groups. During remyelination, the OPC and OL populations were both significantly increased in [CPZ] + 3ND, but not in [CPZ + Rapa] + 3ND. Scale bars: 100 μm. (For interpretation of the references to color in this figure legend, the reader is referred to the web version of this article.)

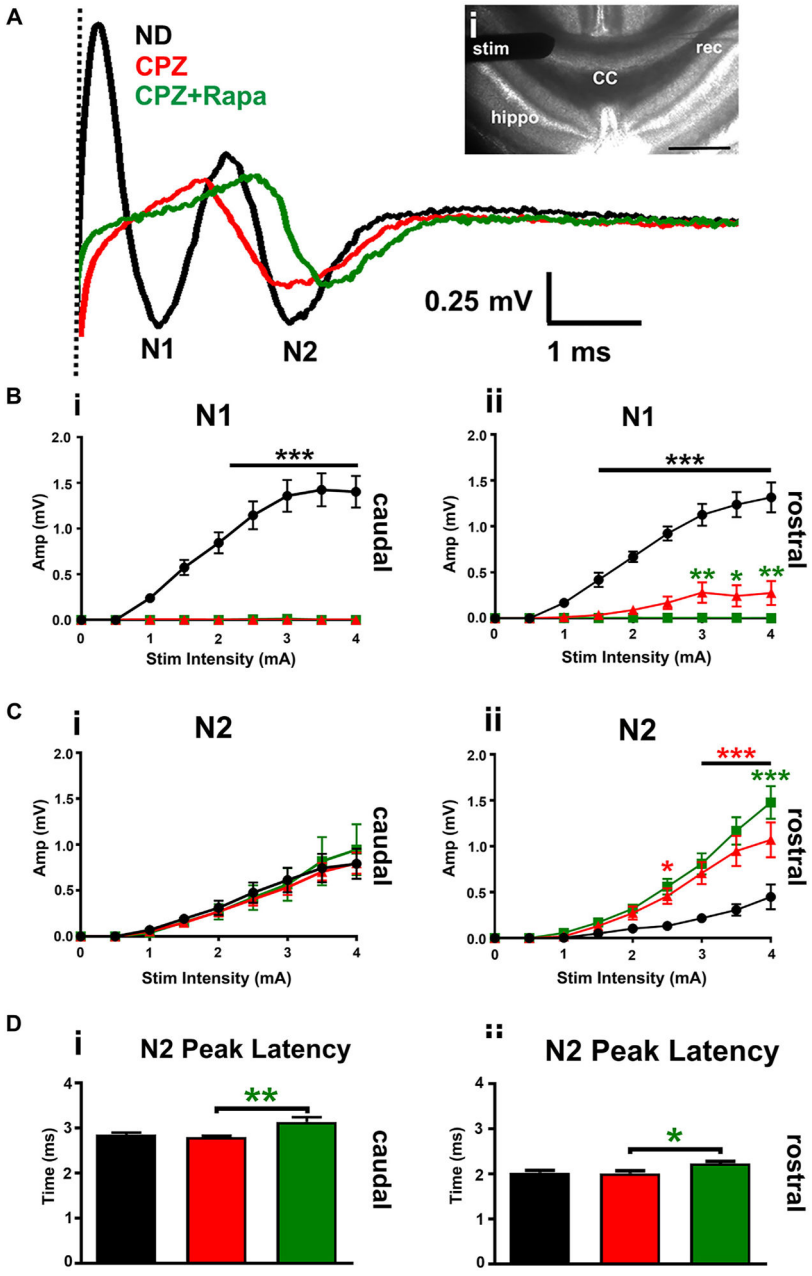

Fig. 9.

Rapamycin increases CC CAP latency and decreases amplitude during demyelination. (A) (i) Recordings were performed across the CC by placing a recording electrode (rec) approximately 1 mm away from a stimulating (stim) electrode, with intensity between 0 and 4 mA. (A) Representative CAP traces at 4 mA from ND, CPZ, and CPZ + Rapa. The dashed line separates the stimulus artifact from the CAP. The ND group has a very pronounced N1 and N2, while the N1 peak for both the CPZ and CPZ + Rapa groups was greatly diminished. (B)The N1 peak amplitude decreased significantly in the CPZ mice compared to ND ($p < 0.001$) for both caudal (i) and rostral (ii) sections, as well as for rapamycin-treated groups compared to non-rapamycin groups in rostral recordings only (ii). No significant

difference was observed between CPZ and CPZ + Rapa for the N1 peak amplitude in caudal section recordings (i). (C) For the unmyelinated axons, no significant change was observed in N2 peak amplitude in caudal sections (i), although an increase in amplitude was seen in rostral recordings for the rapamycin-treated group compared to the non-rapamycin cuprizone group. (D) The latency of the N2 peak was significantly longer for CPZ + Rapa compared to CPZ alone for both caudal (i) and rostral (ii) sections.

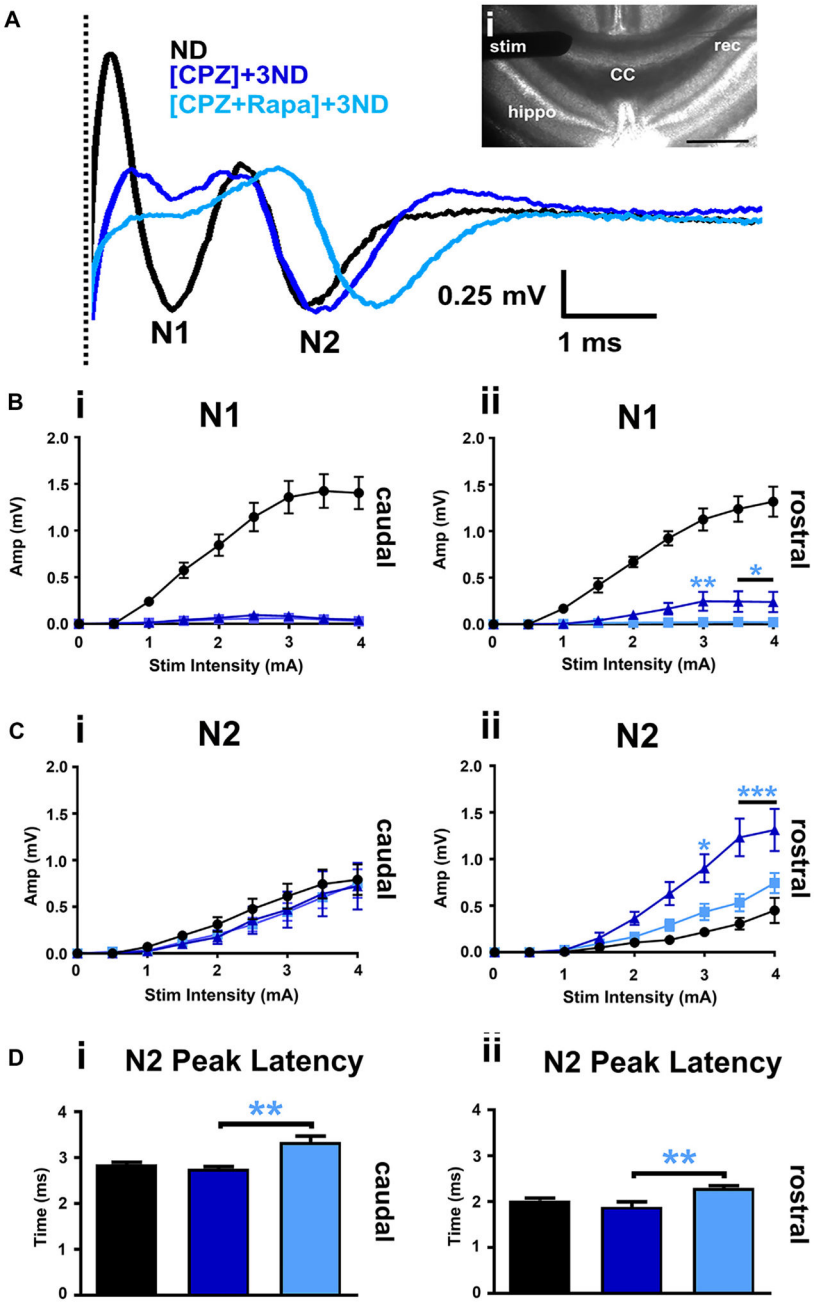

Fig. 10.

Rapamycin during CPZ increases CC CAP latency and decreases amplitude after remyelination. (A) (i) Recordings were performed across the CC by placing a recording electrode (rec) approximately 1 mm away from a stimulating (stim) electrode, with intensity between 0 and 4 mA. (A) Representative CAP traces at 4 mA from ND, [CPZ] + 3ND, and [CPZ + Rapa] + 3ND. The dashed line separates the stimulus artifact from the CAP. There is a pronounced N1 and N2 peak for ND, compared to the [CPZ] + 3ND and [CPZ + Rapa] + 3ND mice which have a similar N2 Peak but relatively diminished N1 Peak. (B) No significant difference was observed in N1 peak amplitude between the [CPZ] + 3ND mice

compared to the [CPZ + Rapa] + 3ND mice in caudal sections (i), although the N1 peak amplitude was significantly lower in the rapamycin-treated remyelination group compared to the non-rapamycin group in rostral sections (ii). (C). Similarly, N2 peak amplitude showed no significant difference in caudal sections (i), with a lower N2 peak amplitude for rapamycin-treated groups in rostral sections (ii). (D) The latency of the N2 peak was significantly longer for [CPZ + Rapa] + 3ND compared to [CPZ] + 3ND for both caudal (i) and rostral (ii) sections, indicating slower axonal conduction.

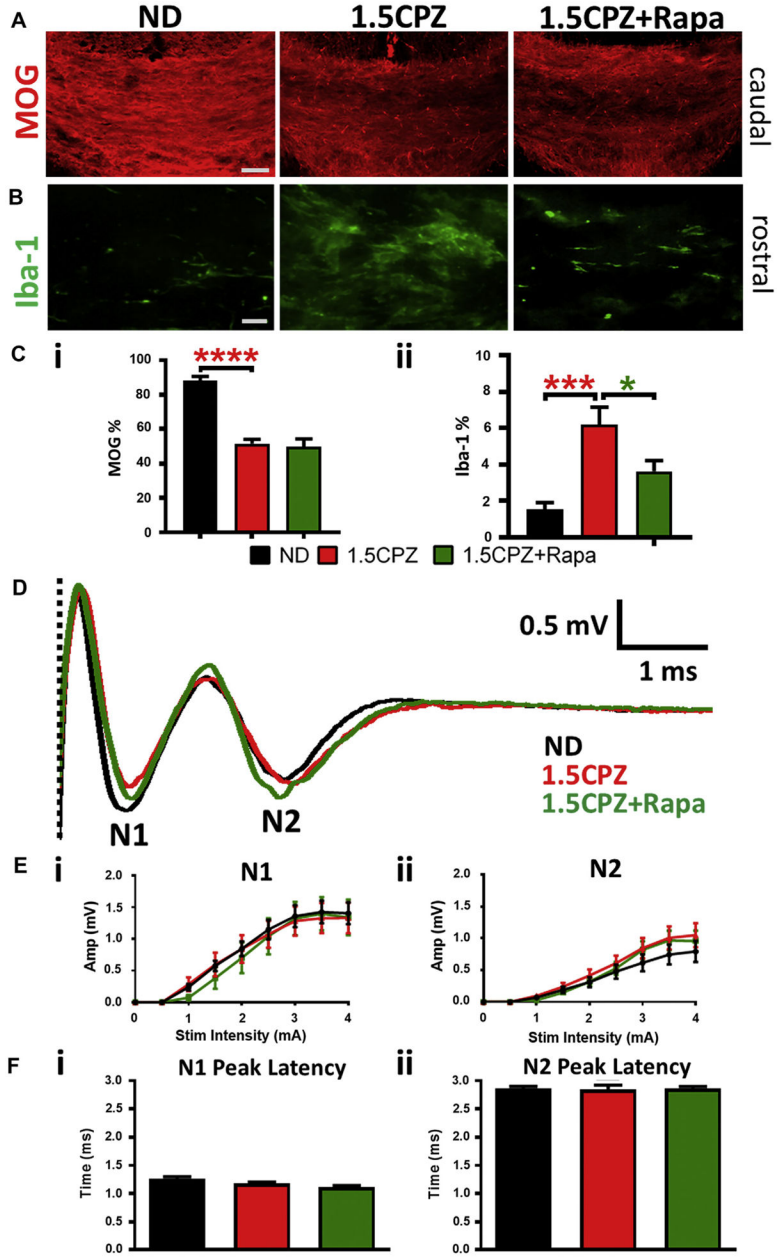

Fig. 11.

Rapamycin administration for 1.5 weeks does not change MOG immunostaining or CAPs but reduces Iba-1 levels in the CC relative to cuprizone diet alone. (A) Representative 10× coronal brain section images of MOG immunostaining in caudal CC sections from ND, 1.5CPZ, and 1.5CPZ + Rapa groups (scale bar: 100 μm), quantified for both rostral and caudal sections in (C) (i). (B) Representative 40× coronal brain section images of Iba-1 immunostaining in rostral CC sections from ND, 1.5CPZ, and 1.5CPZ + Rapa groups (scale bar: 10 μm), quantified for both rostral and caudal sections in (C) (ii). (C) MOG staining intensity (i) decreased during demyelination compared to ND, with no difference observed between Rapa and non-Rapa groups. Iba-1 staining intensity (ii) increased during 1.5CPZ demyelination compared to ND but was reduced in the rapamycin-treated group compared to

1.5CPZ alone. Scale bar: 100 μm. (D) Electrophysiological recordings of CC CAPs at a stimulus strength of 4 mA were recorded from ND, CPZ for 1.5 weeks (1.5CPZ) and CPZ + Rapa for 1.5 weeks (1.5CPZ + Rapa). (E) After 1.5 weeks of demyelination, neither N1 nor N2 peak amplitude showed any statistically significant difference between any groups. (F) The N1 and N2 peak latencies were also not statistically significant between any groups.

Table 1.

Select primary antibodies were used for the examination of myelin, axons, astrocytes, leukocytes, OPCs, and mature OLs, paired with secondary antibodies Alexa Fluor 555 and 647 for immunohistochemistry.

Antibody	Target	Vendor	Catalog #
MBP	Myelin basic protein	Millipore	AB9348
MOG	Myelin oligodendrocyte glycoprotein	Millipore	MAB5680
SMI-32	Unphosphorylated neurofilament H	Millipore	NE1023
GFAP	Glial fibrillary acidic protein; Astrocytes	Zymed	18–0063
CD45	Cluster of differentiation 45; Common leukocyte antigen	BD Pharmingen	BD550539
Iba-1	Ionized binding adaptor molecule-1; Microglia	Wako	019–19,741
Olig2	Oligodendrocytes	Millipore	AB9610
CC1/APC	Mature myelinating oligodendrocytes	Genetex	GTx16794
Ki67	Cell cycle related nuclear protein	Millipore	AB9260